RSC Advances

PAPER

View Article Online
View Journal | View Issue

Cite this: *RSC Adv.*, 2017, **7**, 51919

A highly efficient gas-dominated and water-resistant flame retardant for non-charring polypropylene

Zhu-Bao Shao,[a] Ming-Xin Zhang,[a] Ye Han,*[a] Xu-Dong Yang,[a] Jing Jin[a] and Rong-Kun Jian*[b]

Traditional phosphorus–nitrogen (P–N) flame-retardant systems for polypropylene (PP) always act through joint action of the gaseous phase and condensed phase, and are accompanied with a decrease of the thermal stability and water resistance. In this work, a novel mono-component and gas-dominated flame retardant, named DPPIP, was prepared through an amidation reaction of diphenylphosphinyl chloride and piperazine, and used to flame retard PP. Experimental results confirmed that both the thermal stability and water resistance of PP/DPPIP were improved. The initial thermal decomposition temperature of PP/25 wt% DPPIP at 5 wt% weight loss was 287.5 °C under air atmosphere, which is higher than that of neat PP (266.1 °C). Besides, a water-resistance test verified that PP/25 wt% DPPIP had a weight loss of only about 0.52 wt%. More importantly, the flame retardant ability of PP/25 wt% DPPIP had been greatly improved, passing the V-0 rating (UL-94). Furthermore, after the water-resistance test, the LOI value of PP/25 wt% DPPIP exhibited nearly no difference and still passed the UL-94 V-0 rating. A cone calorimeter (CC) result indicated that DPPIP had a positive effect on inhibiting heat release of PP during combustion. All of these combustion tests displayed that there was no char left. The flame retardant mechanism of DPPIP was investigated with py-GC/MS and TG-FTIR. The results illustrated that the gaseous phase resulting from the thermal decomposition of DPPIP played the leading role in the self-extinguishing behavior of PP/DPPIP, which consisted of a large amount of inflammable gaseous products such as piperazine and its derivatives, and phosphorus-containing structures.

Received 5th September 2017
Accepted 20th October 2017

DOI: 10.1039/c7ra09868e

rsc.li/rsc-advances

1. Introduction

Halogen-free flame retardant systems, such as metal hydroxides, metal borates and intumescent flame retardants (IFR) *etc.*, have been utilized to obtain flame-retardant PP composites.[1–4] Among these halogen-free flame retardant systems, intumescent flame retardants, especially phosphorus–nitrogen (P–N) flame retardants, have attracted much attention in flame-retardant PP due to their high flame-retardant efficiency.[5–7]

In order to obtain better flame-retardant efficiency of PP, a lot of work has been done in past decades, especially research on the flame-retardant mechanism. Generally, traditional P–N flame retardants for PP mainly contain three components, which are an acid source, blowing agent and charring agent,[8,9] and when P–N flame retardants are heated beyond a critical temperature they can generate multicellular swollen chars on the surface of the polymer accompanied by decomposition of the blowing agent, slowing down the heat and oxygen transfer, thus protecting the substrate from burning.[10,11] Therefore, these flame-retardant systems for PP usually act through a gaseous phase and condensed-phase flame-retardant mechanism together. Compared with the production of gas, the condensed-phase formation of P–O–C structures during combustion is one of the methods to improve the flame-retardant efficiency, and the typical flame retardant system is a mixture of ammonium polyphosphate and charring agent (CA).[12–14] Wang *et al.*[15] synthesized a novel charring agent (CA), namely MTEC, and found that a PP/APP/MTEC system could achieve a LOI value of 28.5% and acquire a UL-94 V-0 rating at 20 wt% APP/CA through the formation of P–O–C structures during combustion. The condensed-phase formation of P–N–C structures during combustion is also an efficient method to enhance the flame-retardant efficiency of PP. In our previous papers,[16–18] APPs modified with ethylenediamine (EDA), ethanolamine (ETA) or piperazine (PIP) were incorporated alone into PP. The results also indicated that P–N–C structures were formed during combustion, which could enhance the flame-retardant efficiency for PP. In summary, APP is an essential component to facilitate the formation of stable char during two P–N flame-retardant methods. Unfortunately, the thermal stability and water resistance of APP and modified APPs were not improved

[a]*Institute of Chemical Engineering, Changchun University of Technology, Changchun 130012, China. E-mail: zhu871227@163.com*

[b]*Fujian Key Laboratory of Polymer Materials, College of Materials Science and Engineering, Fujian Normal University, Fuzhou 350007, China. E-mail: jrkht1987@fjnu.edu.cn*

due to the production of large amounts of amine salts and the introduction of organic amine salts. Although lots of work has been done, such as the modification of APP and micro-encapsulated APP,[13,19] these problems still exist, which has limited the application of APP in the practical field. Thus, some researchers have considered whether PP could obtain an excellent efficiency only acting through a gas-dominated flame retardant.

In the present work, a novel mono-component, only gas-dominated and P–N containing flame retardant, named DPPIP, was synthesized through the reaction of diphenylphosphinyl chloride and piperazine, and different measurements were used to confirm its chemical structure. The thermal stability and water resistance of DPPIP were examined. PP/DPPIP blends were prepared *via* physical blending, and their thermal stability, water-solubility and flame retardancy were also studied. Finally, the flame retardant mechanism of DPPIP was investigated with the aid of different measurements.

2. Experimental section

2.1. Materials

Diphenylphosphinyl chloride (DPPC) was supplied by Shanghai Changgen Chemical Reagent Co., Ltd. (Shanghai, China); piperazine (AR), chloroform (AR) and triethylamine (AR) were purchased from Tianjin Kemiou Chemical Reagent Co., Ltd. (Tianjin, China); polypropylene (T30S) was obtained from Petro China Lanzhou Petrochemical Co., Ltd. (Lanzhou, China).

2.2. Measurements

Fourier transform infrared spectroscopy (FTIR) tests were performed on a Nicolet FTIR 170SX spectrometer (Nicolet, America) using a KBr disk, and the wavenumber range was set from 4000–400 cm^{-1}.

^{1}H nuclear magnetic resonance (^{1}H-NMR) spectra and ^{31}P nuclear magnetic resonance (^{31}P-NMR) spectra were recorded on a Bruker AV II-400 MHz spectrometer (Bruker, Switzerland) using $CDCl_3$ as solvent. The sample (85 mg) was put into an NMR tube, then a solution of $CDCl_3$ (5 mL) was injected into the NMR tube, and next the NMR tube was shaken until the solids were dissolved in $CDCl_3$. The concentrations of DPPIP, PIP or DPPC were about 1.7 g/100 mL. The NMR test was performed at about 25 °C, and TMS was applied. The peak which appeared at 0 ppm in the ^{1}H-NMR spectra was ascribed to TMS.

X-ray photoelectron spectroscopy (XPS) spectra were recorded on an XSAM80 spectrometer (Kratos Co, UK) equipped with Al Kα excitation radiation (*hv*-1486.6 eV).

Tensile testing was completed in accordance with the procedures in GB/T 1040.1-2006 at a crosshead speed of 20 mm min^{-1}. The Izod impact properties were tested in accordance with the procedures in GB/T 1843-2008 and the depth of the nick was 2 mm.

Thermogravimetric (TG) analysis was carried out on a TG 209 F1 (NETZSCH, Germany) thermogravimetric analyzer at a heating rate of 10 °C min^{-1} under a nitrogen or air flow of 50 mL min^{-1} in the temperature range from 40 to 700 °C.

The LOI value was measured using an HC-2C oxygen index instrument (Jiangning, China) according to ASTM D2863-97. The sheet dimensions of all of the samples were 130 mm × 6.5 mm × 3.2 mm.

The UL-94 vertical burning level was tested on a CZF-2 instrument (Jiangning, China) according to ASTM D 3801. The dimensions of the samples were 130 mm × 13 mm × 3.2 mm.

The flammability of the samples was measured on a CC device (Fire Testing Technology, UK). Samples with dimensions of 100 mm × 100 mm × 3 mm were exposed to a radiant cone at a heat flux of 50 kW m^{-2}.

The thermogravimetry-Fourier transform infrared spectroscopy (TG-FTIR) apparatus consisted of a TG 209 F1 (NETZSCH, Germany) thermogravimetric analyzer and a 170 SX FTIR spectrometer (Nicolet, America). A sample (about 6 mg) was heated at a rate of 10 °C min^{-1} in the temperature range from 40 to 700 °C under a nitrogen flow of 50 mL min^{-1}.

The samples for the py-GC/MS tests were first pyrolyzed in a pyrolyzer (CDS5200) under helium atmosphere. The relevant samples (300 μg) were heated from ambient temperature to 600 °C at a rate of 20 °C ms^{-1} and kept for 15 s. Then, the volatile products were carried through helium to a Perkin-Elmer Clarus680GC-SQ8MS system coupled with the pyrolyzer. The temperature of the capillary column (HP-5, 0.25 mm) of the GC was held at 40 °C for 3 min; afterward, the temperature was increased to 280 °C at a heating rate of 10 °C min^{-1} and then kept at 280 °C for 5 min. The injector temperature was maintained at 280 °C. The MS indicator was operated in the electron impact mode at an electron energy of 70 eV, and the ion source temperature was kept at 250 °C. The identification of the pyrolysis products was carried out by comparing to the NIST MS library.

The water-resistance of the flame retardant and modified PP was tested according to the following procedure: 10 g of flame retardant was put into 100 mL of distilled water at 70 °C and stirred for 60 min. The suspension was then filtered. Next, the obtained solid was dried to a constant weight at 100 °C. Finally, the solubility of the flame retardant in water was obtained.[20] The modified PP (the weight of M_0) was put into distilled water at 70 °C, and kept at this temperature for 168 h (the water was replaced at each interval of 24 h). Then the treated specimens were taken out, and dried to a constant weight at 100 °C. The weight of the dried sample is M_1, so the weight loss can be calculated based on the following equation: $[(M_0 - M_1)/M_0] \times 100\%$.[20]

2.3. Synthesis of DPPIP

47 g of diphenylphosphinyl chloride and 100 mL of chloroform were mixed in a 250 mL three-necked round-bottom flask equipped with a reflux condenser, dry N_2 inlet, and a dropping funnel. The mixture was agitated in an ice-bath under nitrogen atmosphere. Half an hour later, 8 g of piperazine dissolved in chloroform (20 mL) was added over 1 h. Then 60 g of triethylamine was added to the solution. After completing the addition, the solution was heated to 75 °C for 8 h until the reaction completely finished. Finally, the solution was cooled to room

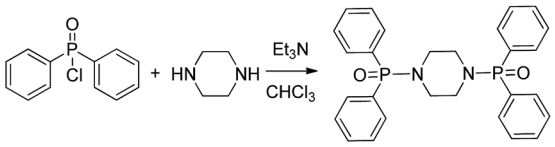

Scheme 1 The synthetic route of DPPIP.

temperature and then filtered. The filtrate was evaporated under reduced pressure to obtain the crude product. The product was washed with water repeatedly to remove the impurities, then dried at 85 °C for 12 h under vacuum to a constant weight (84.3% yield). The reaction formula is described in Scheme 1.

2.4. Sample preparation

DCPIP was dried in a vacuum oven at 85 °C for 12 h. Then PP blends filled with different ratios of DCPIP were prepared *via* a twin-screw extruder (CTE 20, Kebeilong Keya Nanjing Machinery Co., Ltd, Nanjing, China) with a rotation speed of 150 rpm with the following temperature protocol from the feed zone to the die: 175, 180, 190, 185, 180 and 170 °C. Finally, the extruded pellets were hot-pressed into different samples by a plate vulcanizer (Qingdao Yadong Rubber Viachinery Co. Ltd. China).

3. Results and discussion

3.1. Characterization of DPPIP

The FTIR spectrum of DPPIP is shown in Fig. 1. The peaks at around 3025.6–3059.4 cm^{-1} and 760.9 cm^{-1} are ascribed to the C–H vibrations of the benzene rings. The peaks located at 2948.6–2962.8 cm^{-1} are assigned to the C–H stretching vibrations of PIP. The peaks at 1116.4 cm^{-1} and 722.5 cm^{-1} correspond to the P–N–C vibrations,[16–18] and the peak at 1178.8 cm^{-1} is assigned to the P=O vibration. The results show that DPPIP had been prepared successfully.

To confirm the formation of DPPIP, ^{1}H-NMR and ^{31}P-NMR tests of DPPC, PIP and DPPIP were performed, and the results are displayed in Fig. 2. All of the protons can be attributed to the expected signals. Compared with the ^{1}H-NMR spectrum of PIP (Fig. 2b), the N–H signal at 1.75 ppm disappeared and the peak at 2.80 ppm shifted to 3.11 ppm in DPPIP, which is assigned to $-CH_2-$ in the $-CH_2-N-P-$ group, indicating that the P–N bond is formed. In the ^{31}P-NMR spectra, there was only one peak at 44.95 ppm for DPPC, which is ascribed to the P in the –P–Cl group, and DPPIP displayed one characteristic peak at 29.47 ppm, indicating that the P–N bond is formed and a high purity of DPPIP. All of the ^{1}H-NMR and ^{31}P-NMR results demonstrate that DPPIP was obtained successfully.

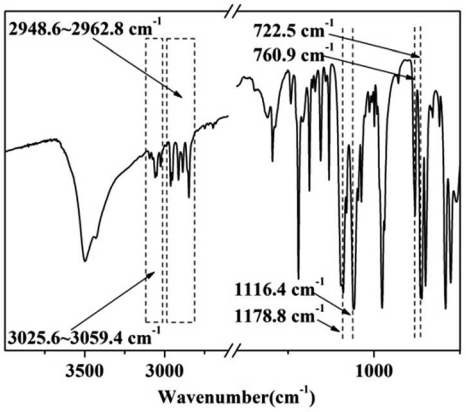

Fig. 1 FTIR spectrum of DPPIP.

To further determine the structure of DPPIP, XPS measurements of PIP and DPPIP were carried out. Their N_{1s} spectra are shown in Fig. 3. For PIP, the peak at 399.2 eV is ascribed to the N in –C–NH–C–.[17] While for DPPIP, a new peak at 402.0 eV is attributed to the N in –P–N–C–, further indicating that DPPIP was formed.

3.2. Water resistance

Water resistance is an important property to assess the usability of flame retardants in polymers. Thus, the water solubility of DPPIP was tested and compared with our previously modified APPs (PA-APP), and the corresponding data are listed in Table 1. It could be observed that PA-APP is easily dissolved in 70 °C water due to the large amount of hydrophilic amine salt, and the water solubility value is 10.0 g/100 mL of water. However, because of the hydrophobic nature of P–N and the benzene rings, the water solubility of DPPIP is less than 0.01 g/100 mL of water. Moreover, the water resistance of PP/DPPIP and PP/PA-APP was also evaluated through water-solubility experiments, and the results are listed in Table 1. For PP/DPPIP, the weight loss is only 0.52 wt%, which is far less than that for PP/PA-APP. These results demonstrate that DPPIP and PP/DPPIP have an excellent water resistance.

3.3. Thermogravimetric analysis

TG and derivative thermogravimetric (DTG) curves of neat PP, DPPIP and PP/DPPIP under N_2 and air atmosphere are illustrated in Fig. 4, and the corresponding data are listed in Table 2. There is only one degradation step for DPPIP ranging from 300–420 °C under N_2 atmosphere, and the initial decomposition temperature ($T_{5\%}$, defined as the temperature where the mass loss is 5 wt%) of DPPIP is 328.9 °C, which is lower than that of neat PP (383.5 °C). Consequently, with the addition of DPPIP, the initial decomposition temperature of modified PP (N_2) decreased, and it corresponds well to that in the calculated curve. However, the degradation of PP/DPPIP under air atmosphere is very different, as the initial decomposition temperature of DPPIP (310.8 °C) is higher than that of neat PP (266.1 °C). As shown in Fig. 4c and d, with the temperature rising, the residues at 700 °C are almost gone for the neat PP, DPPIP and PP/DPPIP both under N_2 and air atmosphere. The TG results suggest that the char layer is not formed at 700 °C, indicating that DPPIP generated almost only gas-phase products during the decomposition.

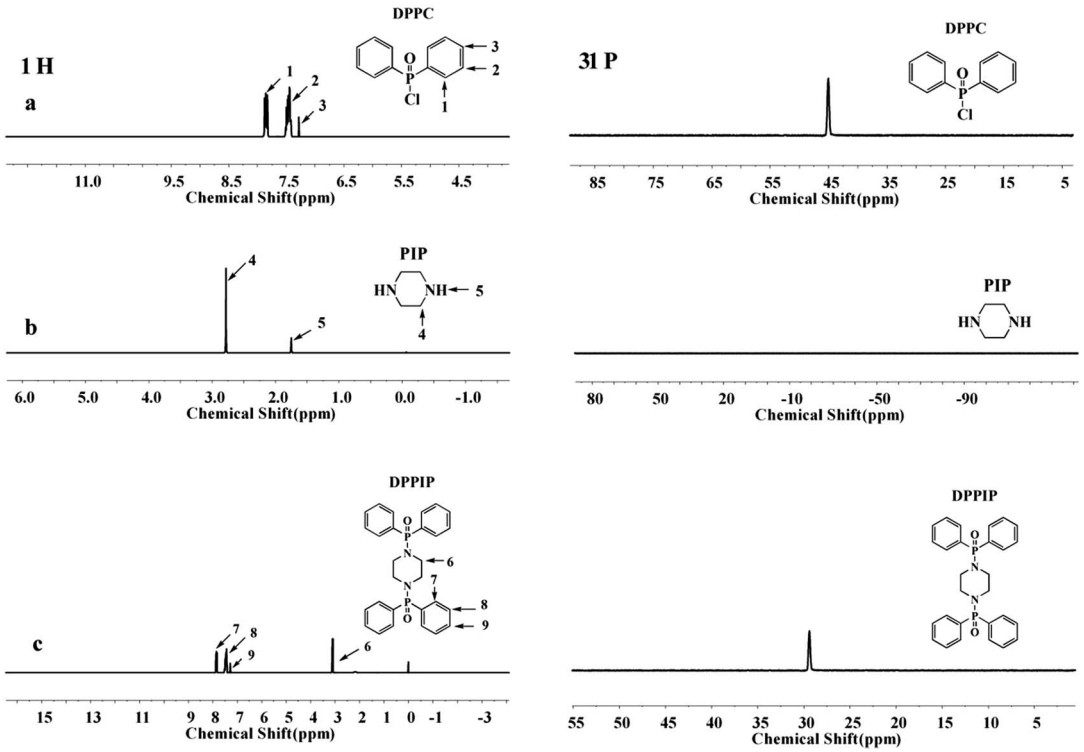

Fig. 2 ^{1}H-NMR and ^{31}P-NMR spectra of DPPC (a), PIP (b) and DPPIP (c).

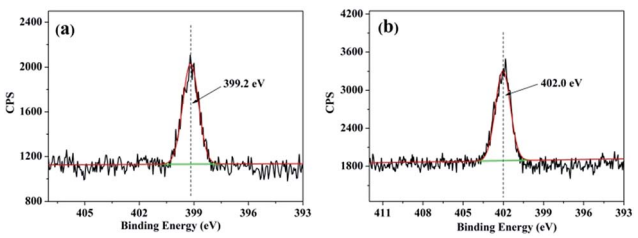

Fig. 3 N_{1s} spectra of PIP (a) and DPPIP (b).

Table 1 Water solubility of DPPIP, PA-APP, PP/DPPIP and PP/PA-APP

Sample	Average water solubility (g/100 mL of water)	Sample	Average weight loss (wt%)
DPPIP	<0.01	PP/25 wt% DPPIP	0.52 ± 0.02
PA-APP	=10.0	PP/25 wt% PA-APP	6.53 ± 0.04

3.4. Mechanical properties of flame-retardant PP composites

The mechanical properties of PP/PA-APP and PP/DPPIP, including the tensile strength, elongation at break, and impact strength, are listed in Table 3. Compared with PP/PA-APP, PP/DPPIP with an equal amount of flame retardant had no apparent change in the impact strength, but both the tensile strength and elongation at break for PP/DPPIP increased. Therefore, it can be concluded that DPPIP is more conducive to the improvement of the mechanical properties of flame-retardant PP than PA-APP.

3.5. Flame retardancy

The flame retardant performances of neat PP and PP/DPPIP before and after water-resistance tests were evaluated by LOI and UL-94 testing, and the corresponding data are listed in Table 4. The two tests showed that neat PP is a flammable polymer. For PP/DPPIP, with an increasing amount of DPPIP,

Table 2 Thermogravimetric properties of PP, DPPIP and PP/DPPIP

	N_2				Air			
		T_{max} (°C)				T_{max} (°C)		
Sample	$T_{5\%}$ (°C)	1	2	Residue (%)	$T_{5\%}$ (°C)	1	2	Residue (%)
Neat PP	383.5	451.9		0.0	266.1	338.4		0.0
DPPIP	328.9	416.3		0.0	310.8	387.3		0.1
PP/25 wt% DPPIP	340.1	404.6	451.0	0.0	287.5	332.1	398.2	0.1
Calculated data	368.0	422.5	452.5	0.0	268.5	340.1	387.5	0.0

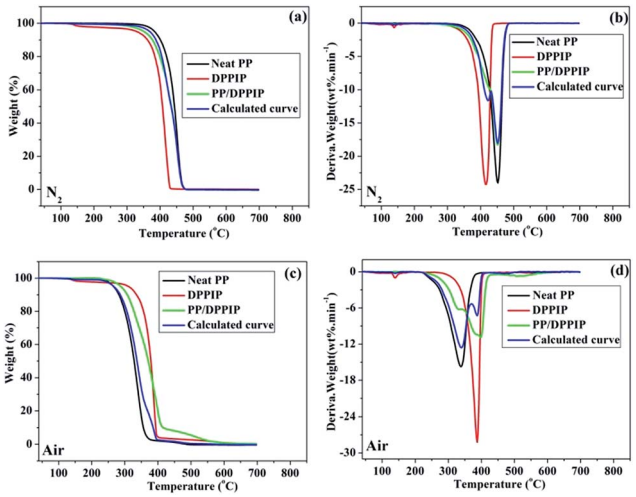

Fig. 4 TG and DTG curves of neat PP, DPPIP, and PP/25 wt% DPPIP and the calculated curve of PP/25 wt% DPPIP at a heating rate of 10 °C min^{-1} under N_2 (a, b) and air (c, d) atmosphere.

the LOI value increased from 18.0% (neat PP) to as high as 28.5% with the addition of 30 wt%. Furthermore, with only 25 wt% addition of DPPIP, the flame-retardant PP can pass the UL-94 V0 rating and dripping is not observed. After the water treatment, the LOI value of flame-retardant PP decreased slightly, and when the addition of DPPIP was 25 wt%, the LOI value decreased from 27.0% to 26.9%, and this can still pass the UL-94 V0 rating. These results indicate that DPPIP is an effective flame retardant for PP, which could further meet the needs of practical application.

CC testing is an effective method to assess the combustion behavior of materials. The corresponding heat release rate (HRR), total heat release (THR), smoke production rate (SPR) and total smoke production (TSP) curves of neat PP and PP/25 wt% DPPIP are shown in Fig. 5 and 6, and the corresponding data are presented in Table 5. As shown in Table 5, the time to ignition (TTI) of the neat PP (20 s) is far lower than that of PP/DPPIP (58 s) due to the early decomposition of neat PP at the beginning of combustion, which is in accordance with the TGA results in air atmosphere. Therefore, the ignition-resistance of the composite is improved. With the addition of DPPIP, both the peak of the HRR (PHRR) and the THR of PP/25 wt% DPPIP decreased compared with those of neat PP, especially for the PHRR, which decreased from 904.4 kW m^{-2} to 487.7 kW m^{-2} with a reduction of 46.1% compared with that of PP, indicating that the presence of DPPIP is favorable to suppress the heat release of neat PP.

Table 4 LOI and UL-94 results of neat PP and PP/DPPIP before and after water resistance testing

Component (wt%)		Not treated with water			After water treatment		
			UL-94 (3.2 mm)			UL-94 (3.2 mm)	
PP	DPPIP	LOI (%)	Rating	Dripping	LOI (%)	Rating	Dripping
100	0	18.0	NR	Yes	—	—	—
80	20	24.5	NR	Yes	—	—	—
75	25	27.0	V0	No	26.9	V0	No
70	30	28.5	V0	No	—	—	—

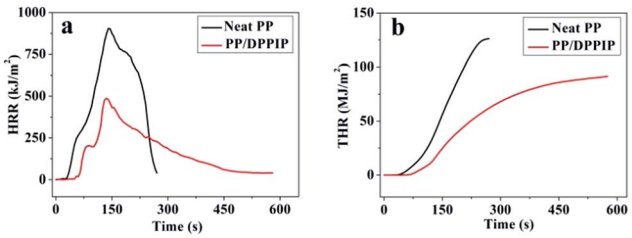

Fig. 5 HRR (a) and THR (b) plots of PP/25 wt% DPPIP.

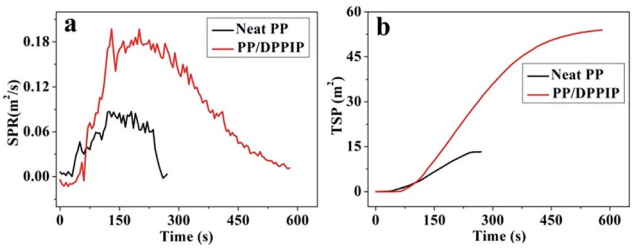

Fig. 6 SPR (a) and TSP (b) plots of PP/25 wt% DPPIP.

Based on the HRR curves, the fire growth rate (FGR) has been calculated to assess the fire hazard of the composite according to the following equation:[21,22]

$$FGR = PHRR/t_{PHRR}$$

Table 3 Mechanical properties of PP/DPPIP and PP/PA-APP

Sample	Flame retardant (wt%)	Tensile strength (MPa)	Elongation at break (%)	Impact strength (kJ m^{-2})
PP/DPPIP	20	38.8 ± 0.3	113.3 ± 5.4	1.83 ± 0.04
	25	33.2 ± 0.2	87.5 ± 6.3	1.95 ± 0.03
	30	29.5 ± 0.3	60.4 ± 4.5	1.98 ± 0.04
PP/PA-APP[17]	20	33.0 ± 0.4	92.4 ± 8.2	1.85 ± 0.02
	25	30.6 ± 0.3	80.7 ± 5.4	1.92 ± 0.03
	30	25.2 ± 0.2	43.2 ± 5.5	2.02 ± 0.03

Table 5 CC data of neat PP and PP/25 wt% DPPIP composites

Sample	Neat PP	PP/DPPIP
TTI (s)	20	58
Peak HRR (kW m^{-2})	904.4	487.7
Time to PHRR (s)	140	135
FGR (kW m^{-2} s)	6.46	3.61
THR (MJ m^{-2})	126.2	87.5
Char residue (wt%)	0.5	1.1

Generally, a lower FGR value indicates that the time to flashover is delayed.[21] For PP/DPPIP, the FGR decreased from 6.46 kW m^{-2} s to 3.61 kW m^{-2} s, which was decreased by 44.1% compared with that of neat PP. This result suggests that the introduction of DPPIP could significantly reduce the FGR of the PP composite, and consequently could significantly extend the time to escape in a real incident.

The SPR and TSP curves of neat PP and PP/DPPIP are presented in Fig. 6, and the corresponding data are summarized in Table 5. It is clear that the SPR and TSP of PP/DPPIP increased more significantly compared with those of neat PP. The results illustrate that PP/DPPIP could produce lots of smoke, and suggest that DPPIP generates gas-phase products during the decomposition.

The digital photos of the residues for neat PP and PP/DPPIP after the CC test are shown in Fig. 7, and the char residues are listed in Table 5. There is almost nothing left after burning, which is in accordance with the TGA results in air and N_2 atmosphere, indicating that the gaseous phase production from the decomposition of DPPIP plays a positive role in the flame retardancy of PP. This can be described as follows: during combustion the decomposition of DPPIP occurs, then a lot of inflammable gas is produced which could dilute the oxygen concentration. As a consequence, the formation of inflammable gas should be the most important factor to achieve a better flame retardancy of PP.

3.6. The flame retardant mechanism of DPPIP

As mentioned above, to reveal the flame-retardant mechanism of DPPIP, the gaseous-phase activity of DPPIP is suggested. Thus, the gaseous phase products of DPPIP were investigated through TG-FTIR, and the FTIR spectra of the gaseous phase products of DPPIP during the thermal decomposition process under N_2 atmosphere are shown in Fig. 8. The absorption peaks of the benzene rings at 3063.3 cm^{-1} and 695.1 cm^{-1} appeared at 328 °C, and some nitrogen-containing and carbon–hydrogen-containing products were released at 328 °C, as they presented the relevant characteristic absorption peaks at 2951.2 cm^{-1} (–CH–, $–CH_2–$, $–CH_3$) and 1437.6 cm^{-1} (–NH–, $–NH_2$). Meanwhile, the absorption peaks at 1246.2 cm^{-1} (P═O), 1125.2 cm^{-1} and 960.6 cm^{-1} (P–C) and 1125.2 cm^{-1} and 727.5 cm^{-1} (P–N–C) appeared.[17,18,23] With increasing time, these absorbing peaks increased in intensity in the range from 328 to 418 °C. The results indicate that some non-flammable volatiles, such as benzene ring containing, nitrogen-containing, carbon–hydrogen-containing and phosphorus-containing products are generated during the thermal degradation of DPPIP.

To further demonstrate the flame retardant mechanism of DPPIP, the prolyzed products of DPPIP were characterized with py-GC/MS measurement and the results are shown in Fig. 9, Table 6 and Scheme 2. It was found that the pyrolysis behavior of DPPIP is very complicated. When DPPIP is heated up to 600 °C, a small molecule like CO_2 is produced at first. With increasing time, more than twenty-three kinds of pyrolysis product were detected, which could be mainly summarized as three kinds of component. The first one was composed of piperazine and its derivatives, including the peaks at 2 (piperazine), 4 (pyrazine), 6 (3-ethylpyrrole), 7 (2-methylpyrazine), 8 ((*E*)-but-2-ene), 11 (2-methylimidazole) and 16 (4,4′-bipyridine), which were obtained from direct breaks of the piperazine ring and its rearrangement into decomposition segments.[23,24] The

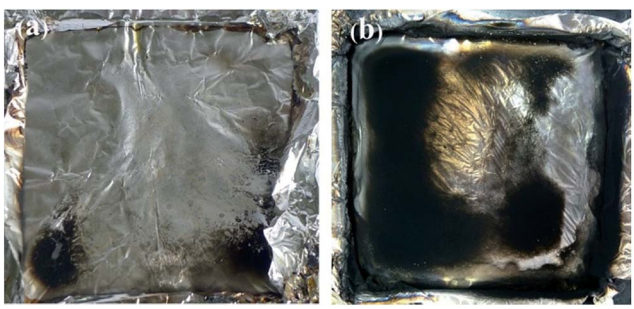

Fig. 7 Digital photographs of residues of neat PP (a) and PP/25 wt% DPPIP (b) composites after the CC test.

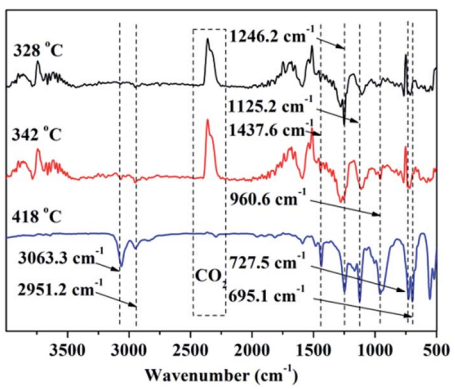

Fig. 8 FTIR spectra of the gaseous products of DPPIP during the thermal degradation under N_2 atmosphere.

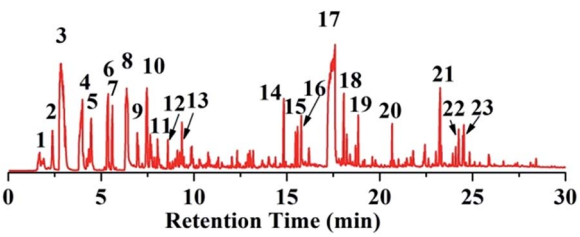

Fig. 9 Pyrograms of DPPIP.

Table 6 Compounds identified from the pyrograms of DPPIP

Peak	Retention time (min)	*m*/*z*	Compounds	Assigned structure
1	1.70	44	Carbon dioxide	O=C=O
2	2.39	86	Piperazine	
3	2.85	78	Benzene	
4	3.99	80	Pyrazine	
5	4.47	92	Toluene	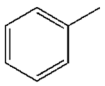
6	5.38	95	3-Ethylpyrrole	
7	5.60	94	2-Methylpyrazine	
8	6.37	56	(*E*)-But-2-ene	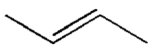
9	6.94	104	Ethenylbenzene	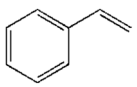
10	7.46	110	Phenylphosphineinhexane	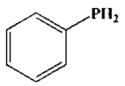
11	7.64	82	2-Methylimidazole	
12	8.03	124	White phosphorus	P_4
13	9.35	107	Methylphenylamine	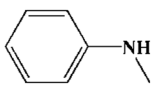
14	14.84	154	Biphenyl	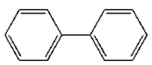
15	15.58	168	2-Methylbiphenyl/4-methylbiphenyl	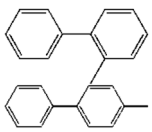
16	15.78	156	4,4′-Bipyridine	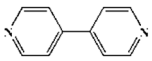
17	17.60	186	Diphenylphosphin	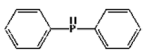
18	18.07	200	Methyldiphenylphosphine	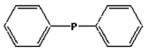
19	18.84	214	Ethyldiphenylphosphine	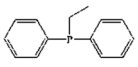
20	20.66	201	Diphenylphosphinoamine	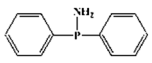

Table 6 (*Contd.*)

Peak	Retention time (min)	*m*/*z*	Compounds	Assigned structure
21	23.25	262	Triphenylphosphine	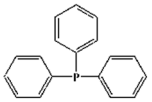
22	24.25	242	Diphenylpropenyl phosphine oxide	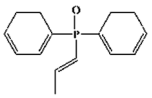
23	25.54	260	Ethylenediamine phosphine oxide	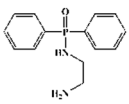

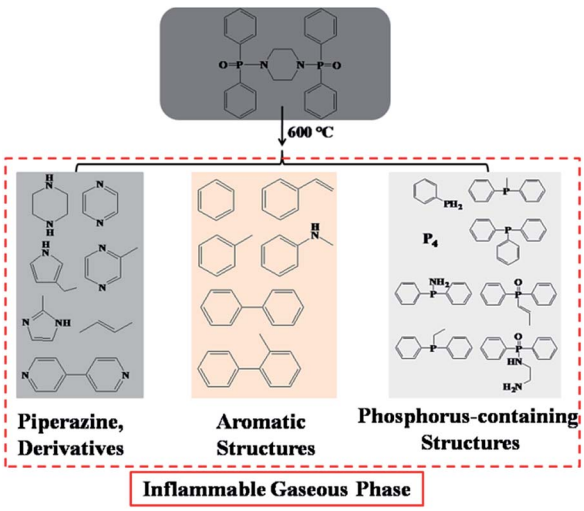

Scheme 2 Speculative pyrolysis products of DPPIP at 600 °C.

second one consisted of the compounds with aromatic structures (peaks at 3, 5, 9, 13, 14 and 15), including the benzene ring and its derivatives. These aromatic derivatives occurred following the rupture of P–Ar. And last, lots of phosphorus-containing structures were detected, corresponding to the peaks at 10, 12, 17, 18, 19, 20, 21, 22 and 23.[24–26] The phosphorus-containing structures could produce PO free radicals to capture active free radicals such as H and hydrocarbon free radicals during combustion.[26] Generally, the result of Py-GC/MS is consistent with those of the TG-FTIR and CC tests.

Based on the Py-GC/MS and FTIR-TG results, the effect of the gaseous phase on the flame retardation of PP is concluded as follows. With increasing temperature, lots of piperazine and its derivatives deriving from direct breaks of the piperazine ring and its rearrangement into decomposition segments are formed and released firstly; meanwhile, the P–Ar bonds break and aromatic structures are produced, which can further increase the amount of inflammable volatile gas. Besides, the rest of the P–Ar bonds continue to be degraded and rearranged, and some structures containing P are finally generated, which can capture active free radicals during the burning.[26] Furthermore, the three kinds of inflammable volatile gases can reduce the oxygen content and capture active free radicals during combustion through the gaseous flame retardance mode, resulting in a superior flame-retardant efficiency of PP.

4. Conclusion

A mono-component flame retardant named DPPIP was prepared in this work. PP/DPPIP showed excellent thermal stability and water resistance: the thermal decomposition temperature of the PP/25 wt% DPPIP composite at 5 wt% weight loss is 287.5 °C under air atmosphere, and the weight loss was only about 0.52 wt% after the water treatment. Meanwhile, PP/DPPIP exhibited excellent flame-retardant efficiency. The LOI value of PP/DPPIP reached 27.0%, and passed the V-0 rating at 25 wt% DPPIP. The CC data showed that the PHRR and low THR *etc.*, especially the FGR, largely decreased compared with the corresponding values of neat PP. Furthermore, there was almost no char residue left. The study on the flame retardant mechanism of DPPIP indicated that lots of inflammable gaseous phase products are produced, such as piperazine and its derivatives, and phosphorus-containing structures, which finally lead to a better flame retardant performance for PP.

Conflicts of interest

There are no conflicts to declare.

Acknowledgements

This work was financially supported by the National Natural Science Foundation of China (grant number 51703011; 21504015; 51603018); Project of Jilin Provincial Department of Education (grant no. 2016329); Program of Jilin Provincial Department of Science & Technology (grant no. 20170520125JH); and Natural Science Foundation of Fujian Province of China (grant number 2015J05094).

References

1 K. C. Mai, Z. J. Li, Y. X. Qiu and H. M. Zeng, *J. Appl. Polym. Sci.*, 2001, **80**, 2617–2623.
2 J. Z. Liang, J. Q. Feng, C. P. Tsui, D. F. Liu, S. D. Zhang and W. F. Huang, *Composites, Part B*, 2015, **71**, 74–81.
3 X. L. Chen, J. Yu, M. He, S. Y. Guo, Z. Luo and S. J. Lu, *J. Polym. Res.*, 2009, **16**, 357–362.
4 Q. H. Tang, R. J. Yang, Y. Song and J. Y. He, *Ind. Eng. Chem. Res.*, 2014, **53**, 9728–9737.
5 Y. Liu, C. L. Deng, J. Zhao, J. S. Wang, L. Chen and Y. Z. Wang, *Polym. Degrad. Stab.*, 2011, **96**, 363–370.
6 X. J. Lai, S. Tang, H. Q. Li and X. R. Zeng, *Polym. Degrad. Stab.*, 2015, **113**, 22–31.
7 H. L. Xie, X. J. Lai, R. M. Zhou, H. Q. Li, Y. J. Zhang, X. R. Zeng and J. H. Guo, *Polym. Degrad. Stab.*, 2015, **118**, 167–177.
8 G. Camino, N. Grassie and I. McNeill, *J. Polym. Sci., Polym. Chem. Ed.*, 1978, **16**, 95–106.
9 Y. L. Wang, X. M. Zhang, A. Li and M. Li, *Chem. Commun.*, 2015, **51**, 14801–14804.
10 M. C. Yewa, N. H. Ramli Sulong, M. K. Yew, M. A. Amalina and M. R. Johan, *Prog. Org. Coat.*, 2015, **81**, 116–124.
11 C. Y. Luo, J. D. Zuo, F. Q. Wang, Y. C. Yuan, F. Lin, H. H. Huang and J. Q. Zhao, *Polym. Degrad. Stab.*, 2016, **129**, 7–11.
12 Z. Z. Xu, J. Q. Huang, M. J. Chen, Y. Tan and Y. Z. Wang, *Polym. Degrad. Stab.*, 2013, **98**, 2011–2020.
13 K. Yang, M. J. Xu and B. Li, *Polym. Degrad. Stab.*, 2013, **98**, 1397–1406.
14 P. Y. Wen, X. M. Feng, Y. C. Kan, Y. Hu and R. K. K. Yuen, *Polym. Degrad. Stab.*, 2016, **134**, 202–210.
15 Z. J. Wang, Y. F. Liu and J. Li, *ACS Sustainable Chem. Eng.*, 2017, **5**, 2375–2383.
16 Z. B. Shao, C. Deng, Y. Tan, M. J. Chen, L. Chen and Y. Z. Wang, *Polym. Degrad. Stab.*, 2014, **106**, 88–96.
17 Z. B. Shao, C. Deng, Y. Tan, M. J. Chen, L. Chen and Y. Z. Wang, *ACS Appl. Mater. Interfaces*, 2014, **6**, 7363–7370.
18 Z. B. Shao, C. Deng, Y. Tan, L. Yu, M. J. Chen, L. Chen and Y. Z. Wang, *J. Mater. Chem. A*, 2014, **2**, 13955–13965.
19 H. J. Lin, H. Yan, B. Liu, L. Q. Wei and B. S. Xu, *Polym. Degrad. Stab.*, 2011, **96**, 1382–1388.
20 C. L. Deng, C. Deng, J. Zhao, R. M. Li, W. H. Fang and Y. Z. Wang, *Chin. J. Polym. Sci.*, 2015, **33**, 203–214.
21 H. Breulet and T. Steenhuizen, *Polym. Degrad. Stab.*, 2005, **88**, 150–158.
22 Y. W. Yan, L. Chen, R. K. Jian, S. Kong and Y. Z. Wang, *Polym. Degrad. Stab.*, 2012, **97**, 1423–1431.
23 *Thermal and fire performance of flameretarded epoxy resin: investigating interaction between resorcinol bis(diphenyl phosphate) and epoxin nanocomposites*, ed. C. Katsoulis, E. Kandare, B. K. Kandola, T. R. Hull and B. K. Kandola, Royal Society of Chemistry, Cambridge, 2009, vol. 17, pp. 184–205.
24 L. P. Dong, C. Deng, R. M. Li, Z. J. Cao, L. Lin, L. Chen and Y. Z. Wang, *RSC Adv.*, 2016, **6**, 30436–30444.
25 L. P. Dong, C. Deng and Y. Z Wang, *Polym. Degrad. Stab.*, 2017, **135**, 130–139.
26 R. K. Jian, P. Wang, W. S. Duan, J. S. Wang, X. L. Zheng and J. B. Weng, *Ind. Eng. Chem. Res.*, 2016, **55**, 11520–11527.